ICIC Express Letters
Part B: Applications
Volume **11**, Number **9**, September **2020**

ICIC International ©2020 ISSN 2185-2766
pp. 875–880

FOCUS MEASURE OF TUNNEL IMAGES

Hea In Jeong and Young Ju Jeong

Department of Computer Science
Sookmyung Women's University
100, Cheongpa-ro 47-gil, Yongsan-gu, Seoul 04310, Korea
{ heain; yjeong }@sookmyung.ac.kr

Received March 2020; accepted June 2020

Abstract. *The features of tunnels hinder distinguishing in-focus photographs taken in tunnels. Focused tunnel images are required for extracting meaningful information about tunnels such as cracks. In this paper, we propose a new focus algorithm induced by commonly used algorithms and suggest a pre-processing phase. The effectiveness of the suggestion is proven by the experimental results from actual tunnel images.*
Keywords: Image processing, Focus measure, Autofocus, Sharpness measure

1. **Introduction.** Autofocus has been used as a fundamental technology in different fields of study [1,2], where defocused images inherently have less information compared to sharply focused images [3]. Image acquisition system with high quality autofocus is essential to obtain accurate information about images and several focus algorithms have been devised for better performance. However, most focus algorithms do not guarantee high performance when used for tunnel images, where most of them consist of walls without objects that are difficult to apply for the existing methods. The image quality depends on the level of focus; a proper sharpness measurement for tunnel images is needed. In this paper, we propose a measurement model for images obtained from tunnels.

Autofocus methods are divided into two systems: Active and Passive. Active system estimates the distance between the lens of the camera and the object of interest using external sensors, and it adjusts the lens position. Active focus method is usually found in professional applications; however, due to high reflectivity of sensor, it could cause difficulty when focusing through window or glass [4]. On the other hand, a passive system determines the position of the lens only based on the information gained from images, which is cost-effective. As a result, this method is deployed in a low-cost consumer-level digital camera.

The passive autofocus system consists of three components: focusing region selection, sharpness measurement, and peak search [5]. Among them, the most widely used image quality factor is the sharpness measure, where it determines the amount of detail in images to obtain more information from high-quality images.

In this paper, we suggest a sharpness measurement which is applicable to tunnel images and review existing sharpness measurement functions such as the Tenengrad and Laplacian measures.

2. **Focus Algorithm.** Recently, many sharpness functions have been suggested and compared. The output of an ideal focus algorithm is defined as having a maximum value at the best focused image/position and decreasing as defocus increases [6]. In this section, four methods were compared and each method is briefly described below.

DOI: 10.24507/icicelb.11.09.875

2.1. **Tenengrad [3].** One of the most widely used measures, Tenengrad convolves the image with vertical (S_x) and horizontal (S_y) Sobel operators. To get a global measure over the whole image, the square of the gradient vector components is summed. It is computed as follows:

$$F_{Tenengrad} = \sum_{x=1}^{M} \sum_{y=1}^{N} S_y(x,y)^2 + S_y(x,y)^2 \tag{1}$$

for an $M \times N$ image block.

2.2. **Sum Modified Laplacian (SML) [7,8].** This method is based on the linear differential operator Laplacian. It has the same properties in all directions invariant to rotation. The difference between SML and Laplacian is that SML is summed with the absolute values of the convolution of the image, where Laplacian is summed with their actual values. The SML is shown as follows:

$$F_{SML} = \sum_{x=1}^{M} \sum_{y=1}^{N} |L_x(x,y)| + |L_y(x,y)| \tag{2}$$

2.3. **Energy of Laplacian (EOL) [9].** This algorithm follows the similar basis with the SML. The difference is that this method convolves an image with a different mask for computation. The sum of the squares of the convolution results is used as the contrast measurement. The EOL is formulated as follows:

$$F_{EOL} = \sum_{x=1}^{M} \sum_{y=1}^{N} D(x,y)^2 \tag{3}$$

where $D(x,y)$ is the second derivative. Several Laplacian masks can be applied, and masks implemented below are typically used.

$$\begin{pmatrix} 0 & -1 & 0 \\ -1 & 4 & -1 \\ 0 & -1 & 0 \end{pmatrix} \begin{pmatrix} -1 & -1 & -1 \\ -1 & 8 & -1 \\ -1 & -1 & -1 \end{pmatrix} \begin{pmatrix} -1 & -4 & -1 \\ -4 & 20 & -4 \\ -1 & -4 & -1 \end{pmatrix} \tag{4}$$

2.4. **Normalized variance [7].** This measure compensates for the differences in average image intensity among different images. The variance of image gray levels is used as a simple but effective contrast measurement.

3. **Image Pre-Processing.** The existing focus measurements are unsuitable for tunnel images, where the most images consist of walls without objects having difficulty to be applied for the existing methods. To improve this issue, a different way to measure the focus of the image for tunnels is required.

Before measuring the sharpness, the image is cropped based on where the object is located. To determine where the object is, interest point features are detected by Speed-Up Robust Feature (SURF) [10]. SURF algorithm can extract features while improving speed over Scale-Invariant Feature Transform (SIFT) [11]. The frequency of the keypoints detected by SURF is calculated and it is assumed that an object exists where the keypoints are clustered. The part of existing objects is cropped to be used as an input for sharpness measure. If the keypoints do not exist, the center of the image is used to measure the focus of images.

Three parameters are prepared to measure the relative degree of focus of images: Tenengrad, Sum Modified Laplacian, and Energy of Laplacian. The performance of normalized variance was not sufficient to measure whether the image is focused or not. Normalization

is required for each measurement due to a different range. The normalization of image size and range of each measurement is performed as:

$$\overline{F_{Tenengrad}} = \frac{F_{Tenengrad} - \mu_{Ten}}{X_{\max} - X_{\min}} \times \frac{1}{M \times N} \tag{5}$$

$$\overline{F_{SML}} = \frac{F_{SML} - \mu_{SML}}{X_{\max} - X_{\min}} \times \frac{1}{M \times N} \tag{6}$$

$$\overline{F_{EOL}} = \frac{F_{EOL} - \mu_{EOL}}{X_{\max} - X_{\min}} \times \frac{1}{M \times N} \tag{7}$$

where $X_{\max}$ and $X_{\min}$ are the maximum and minimum of each method for $M \times N$ image. μ_{Ten}, μ_{SML}, and μ_{EOL} are the average of Tenengrad, SML, and EOL measured in different lens focus, respectively. Using the normalized methods above, the focus measure for tunnel images can be computed as:

$$F_{Tunnel} = 3 \times \overline{F_{Tenengrad}} + \overline{F_{SML}} + \overline{F_{EOL}} \text{ for } F_{Tunnel} > T \tag{8}$$

where T is the threshold.

4. **Experimental Results.** The tunnel images from five different positions were utilized as shown in Figure 1. For each position, more than 350 images were taken in different lens focus. Position 1 is the image of a ceiling in a tunnel and consists of 662 images. Position 4 and Position 5 are left and right side of a tunnel, respectively. 339 images were taken for Position 4 and 313 images for Position 5. Position 2 is the image of location between Position 1 and Position 5 and it consists of 480 images. Position 3 is the image between Position 1 and Position 4. 395 images were taken for Position 3.

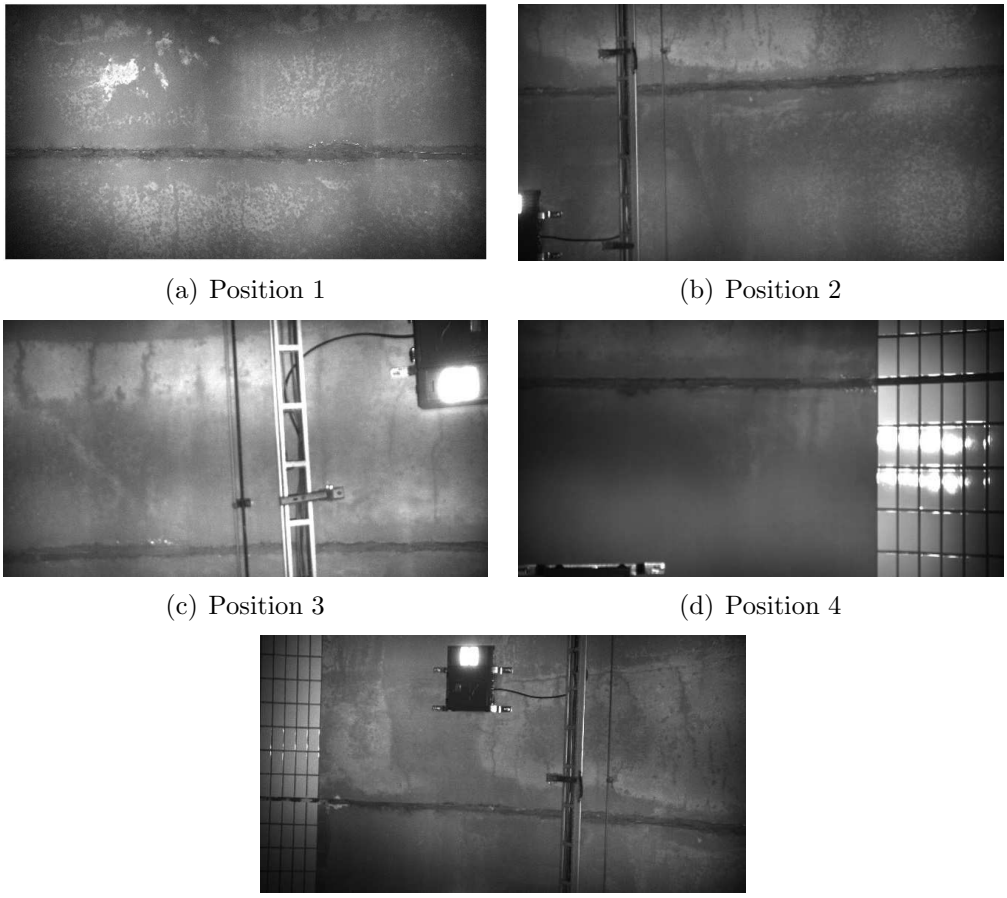

(a) Position 1 (b) Position 2

(c) Position 3 (d) Position 4

(e) Position 5

FIGURE 1. Tunnel images taken at five different positions

Only one image per position was used as an input for keypoint detection. The keypoints detected by SURF were drawn in the image as shown in Figure 2. The images at each position were cropped based on the frequency of the keypoints.

With images taken in five positions, a sharpness graph can be generated from each position. It displays the image index number along the X-axis and the normalized sharpness value (F_{Tunnel}) for each image along the Y-axis. A higher value represents that the image is more in focus. Figure 3 shows the sharpness graph in five different positions. For the

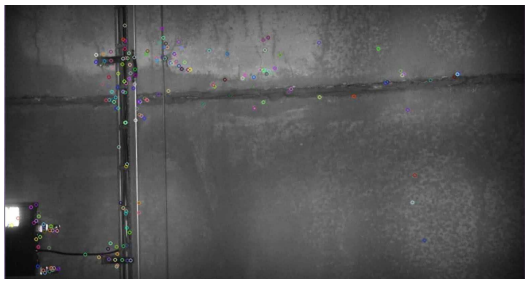

FIGURE 2. SURF keypoint detection of the tunnel image

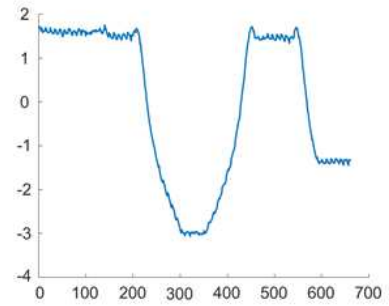

(a) Position 1

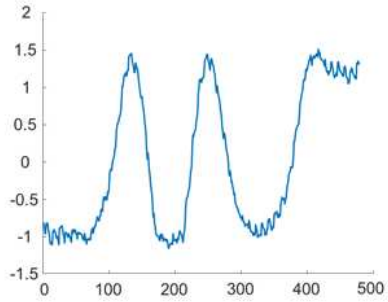

(b) Position 2

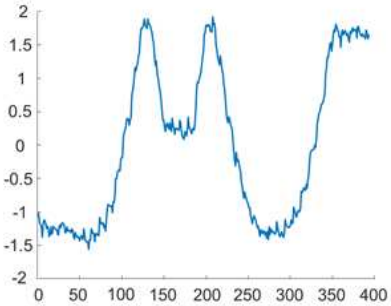

(c) Position 3

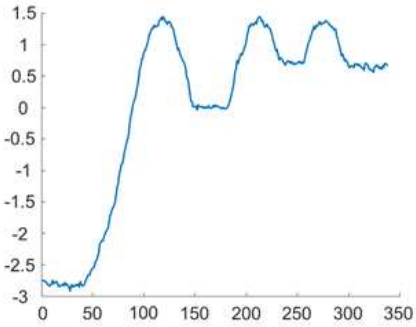

(d) Position 4

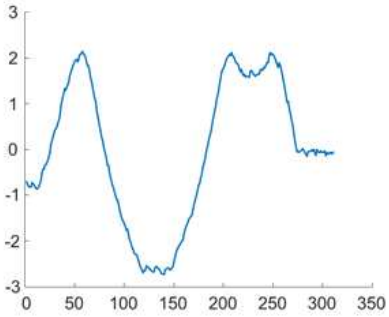

(e) Position 5

FIGURE 3. Sharpness measure graph in different positions

experiment, the threshold is set as 1. If the sharpness value is higher than 1, it is assumed to be in focus.

As seen in Figure 4, an image with larger sharpness value was more in focus than the smaller one. The images with sharpness smaller than threshold could be seen to be out of focus. Images in Figure 4 were both taken at Position 2, with different lens focus. To see whether the images were in focus or not, the image at the bottom right is a magnified version of a crack in the image. Figure 4(b) seemed to be blurry than Figure 4(a).

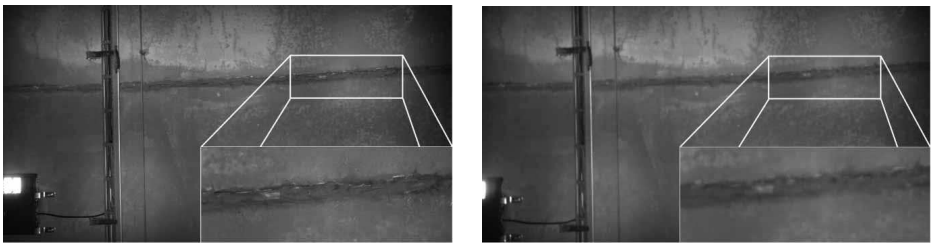

(a) (b)

FIGURE 4. The image in focus and out of focus: F_{Tunnel} of (a) is 1.148 and F_{Tunnel} of (b) is -1.21

With the sharpness graph in Figure 3, the image with a maximum F_{Tunnel} per position was expected to be the most focused image. To determine whether an image with a maximum F_{Tunnel} is the most focused one, Figure 5 showed the images with maximum F_{Tunnel} per position. Figure 5(a) shows an image number 437 in Position 1. Figures 5(b)-5(e) are image number 407, 126, 125, and 221 for Positions 2, 3, 4, and 5, respectively.

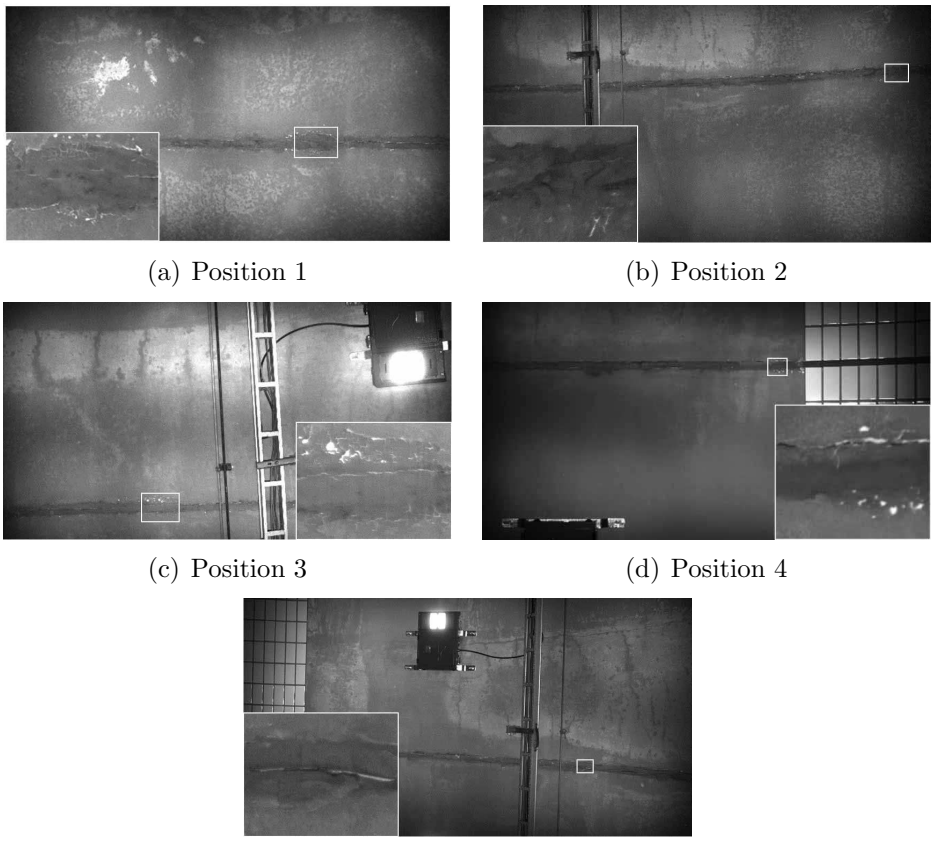

(a) Position 1 (b) Position 2

(c) Position 3 (d) Position 4

(e) Position 5

FIGURE 5. Images with a maximum F_{Tunnel} per position

5. **Conclusions.** In this work, we described an image pre-processing process and a focus measure for tunnel images. As most tunnel images have homogeneous regions, the most widely used focus measures did not show high performance. To solve this issue, we suggested the SURF process before applying focus measure in tunnel images and proposed a new focus algorithm specially targeted tunnel images by comparing four common methods: Tenengrad, Sum Modified Laplacian, Energy of Laplacian, and Normalized Variance. The keypoints of tunnel images were detected by SURF to determine the location of objects in the image. The images were cropped based on the objects and used as an input for focus measurement. The experiment showed five different positions in one tunnel and measured the focus to select the most focused image. The new focus algorithm for the tunnel images showed improved performance compared with the maximum value of the measurement and the tunnel image.

REFERENCES

[1] M. A. Bueno-Ibarra, Fast autofocus algorithm for automated microscopes, *Opt. Eng.*, vol.44, no.6, 2005.
[2] K. De and V. Masilamani, Image sharpness measure for blurred images in frequency domain, *Procedia Engineering*, vol.64, pp.149-158, 2013.
[3] E. Krotkov, Focusing, *Int. J. Comput. Vision*, vol.1, no.3, pp.223-237, 1988.
[4] N. Kehtarnavaz and H. J. Oh, Development and real-time implementation of a rule-based auto-focus algorithm, *Real-Time Imaging*, vol.9, no.3, pp.197-203, 2003.
[5] L. Shih, Autofocus survey: A comparison of algorithms, *P. Soc. Photo-Opt. Ins.*, vol.6502, 2007.
[6] Y. Sun, S. Duthaler and B. J. Nelson, Autofocusing algorithm selection in computer microscopy, *2005 IEEE Int. C. Int. Robot*, pp.70-76, 2005.
[7] F. C. Groen, I. T. Young and G. Ligthart, A comparison of different focus functions for use in autofocus algorithms, *Cytometry*, vol.6, no.2, pp.81-91, 1985.
[8] S. K. Nayar and Y. Nakagawa, Shape from focus, *IEEE T. Pattern Anal.*, 1989.
[9] M. Subbarao and J. K. Tyan, Selecting the optimal focus measure for autofocusing and depth-from-focus, *IEEE T. Pattern Anal.*, vol.20, no.8, pp.864-870, 1998.
[10] H. Bay, T. Tuytelaars and L. Van Gool, SURF: Speeded up robust features, *9th European Conference on Computer Vision (Computer Vision – ECCV 2006)*, pp.404-417, 2006.
[11] D. G. Lowe, Distinctive image features from scale-invariant keypoints, *Int. J. Comput. Vision*, vol.60, no.2, pp.91-110, 2004.